Scale Effect of Spherical Projectiles for Stabilization of Oblique Detonation Waves

Shinichi Maeda, Satoshi Sumiya and Jiro Kasahara
Department of Engineering Mechanics and Energy, University of Tsukuba
1-1-1 Tennodai, Tsukuba, Ibaraki, 305-8573, Japan

Akiko Matsuo
Department of Mechanical Engineering, Keio University
3-14-1 Hiyoshi, Kohoku-ku, Yokohama, 223-8522, Japan

1 Introduction

Detonation initiations and stabilizations by projectiles [1, 2] have been conducted as fundamental studies of combustion processes in a ram-accelerator [3] and an oblique detonation wave (ODW) engine [4]. Lee [5] and Vasiljev [6] formulated the relationship between the required mixture condition (cell size) for the initiation and the projectile velocity (Mach number), by correlating the energetic requirement for the direct initiation of the detonation wave and the energy input into the mixtures by the drag force of the projectile. Higgins and Bruckner [7] experimentally validated this initiation criticality under the projectile velocity was below to slightly above the Chapman-Jouguet (C-J) velocity of the detonable mixture. Kasahara et al. [8] extended the projectile velocities through approx. 1.8 times the C-J velocity. They concluded that the criticality to stabilize a detonation wave, i.e., the stabilized ODW, was almost constant against the projectile velocities. This indicates that the proper local conditions (such as the curvature radius of the detonation wave) are also required for the stabilization, in addition to the energetic requirement for the initiation, which becomes easier to attain as the projectile velocity is increased.

Several previous studies [9-12] investigated such local conditions by calculating the distributions of the induction times or lengths behind a shock wave around a projectile. For the conditions slightly below the stabilization criticality, some visualization studies showed the possibilities of unsteady propagation regimes [8, 9, 13] in which the Deflagration to Detonation Transition (DDT) occurred behind the bow shock around the sphere projectile. Our previous studies [14, 15] revealed the propagation mechanisms and wave structures of unsteady regimes via high time-resolution Schlieren visualizations using a high-speed camera. Although these unsteady regimes were dominated by the complex and unstable DDT process, the stabilized ODWs were dominated by the continuous direct initiation of the overdriven detonation by the projectile and the attenuation of it by the expansion waves [13]. The stabilized ODWs are inherently three-dimensional conical geometries, and have finite curvature radiuses. Our previous studies [15-17] showed that the detonation wave near the projectile was attenuated below (0.8-0.9 times) the C-J velocity by the curvature effect before the wave velocity asymptotically reached the C-J velocity at far field. We proposed that the curvature radius of the

Correspondence to: shinichi_maeda@mech.saitama-u.ac.jp

detonation wave had to be large enough compared to the chemical length scale (represented by the cell width) where the wave velocity had the local minimum value below the C-J velocity for sustaining the conical ODW. And the critical wave curvature radius was quantified for sustaining the curved detonation wave. However, such the stabilization conditions of ODWs around projectiles have not been discussed comparing the different projectile scales.

In the present study, we launched smaller spherical projectiles than we had used [8, 14-17]. We investigated the scale effects of the projectiles for the curvature effect, critical curvature radius and the criticality for stabilizing the ODW comparing with the results of our previous studies.

2 Experimental Setup and Conditions

The experimental setup was nearly identical to that used in our previous studies [8, 14-17], therefore, only the essentials are given here. The two-stage light-gas gun launched the projectile with velocities 2000m/s to 2500m/s into the detonable mixture. The projectile velocities were about 1.2-1.4 times the C-J velocity of the mixtures. The observation chamber that filled with the detonable mixture had glass windows for optical access. A Schlieren system and high-speed camera (HPV-1, Shimadzu) visualized the flowfields. The visualized region was located about 400 mm downstream of a Mylar diaphragm (12-μm thickness) dividing the detonable mixture from the gas gun. The high-speed camera recorded with a 1-μs frame speed, 250-ns exposure time, 312 × 260 spatial resolutions, and 100 continuous frames. The projectile was a sphere made of high-density polyethylene. It had a 3.18-mm dia. which was 0.67 times that used in our previous studies (4.76-mm dia.) [8, 14-17]. In this paper, these are denoted as the «small» or «large» projectiles. The diameter of the observation chamber was considerably larger (approx. 100 times the diameter of the small projectiles) to avoid the influence of wall reflections on the phenomena.

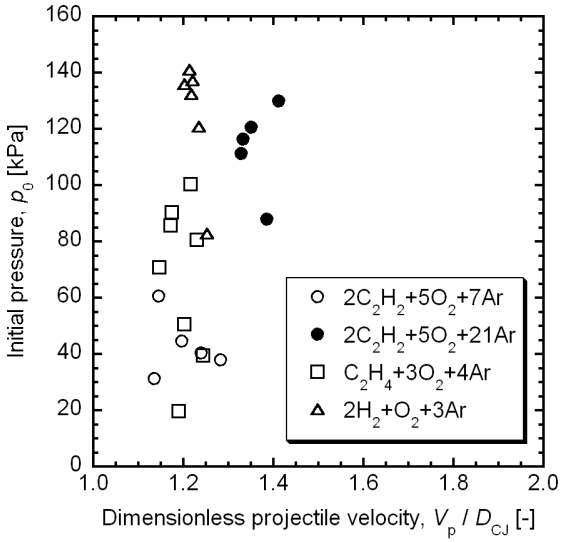

Figure 1. Experimental conditions.

The detonable mixtures were the same as that used in our previous study [17]. They were stoichiometric oxygen mixtures with acetylene, ethylene or hydrogen. Each mixture was diluted with argon in a 50% volumetric fraction to make the C-J velocity lower than the projectile velocity. For the acetylene/oxygen mixture, a 75% dilution was also tested. The projectile velocities and detonabilities of the mixtures are expressed by the dimensionless projectile velocity (V_p / D_{CJ}, V_p: projectile velocity, D_{CJ}: C-J velocity) and filling pressure or dimensionless projectile diameter (d / λ, d: projectile diameter, λ: cell size) as used in previous studies [5, 7, 8, 14-17]. The detonabilities were controlled by varying the filling pressures, and are represented by the cell sizes (widths) accessed from the CALTECH database [18]. For each mixture, fitting equations for cell sizes as an exponential of filling pressures were used to interpolate or extrapolate for each experimental condition. The C-J velocities were calculated by STANJAN [19]. The projectile velocities were determined using dozens of continuous pictures from the high-speed camera. The projectile locations were situated almost linearly over time, and thus velocity deficits in the visualized region were negligible. The experimental conditions are graphically shown in figure 1.

3 Results and Discussion: Observed combustion regimes

First, we show the trends of the observed combustion regimes for the variable filling pressures. Figure 2 shows the example snapshots in $2H_2+O_2+3Ar$ mixture using the small projectiles with the almost constant V_p / D_{CJ} condition (V_p / D_{CJ} = 1.24 ± 0.03). Observed combustion regimes are

represented in figure 3 for the small and large projectiles. The filling pressures decreased from figure 2(a) to (d). Figure 2(a) is the ODW that are characterized by the continuous direct initiation at the projectile front and decay to the C-J detonation at far field. Figure 2(b) and (c) are called Straw Hat type with (b) a stabilized ODW and (c) an attenuated ODW which is characterized by the deflagration to detonation transition behind the bow shock and unsteady propagation of the ODW [14, 15]. Figure 2(d) is the bow shock and shock-induced combustion in which no oblique detonation wave is observed. The qualitative trend was almost the same as that in our previous study [15] using the large projectile. However, the initial pressures for each combustion regime were quantitatively different for the different projectile scales. The small projectile needed higher initial pressure (about 140kPa) to stabilize the ODW than that of the large projectile (about 100kPa).

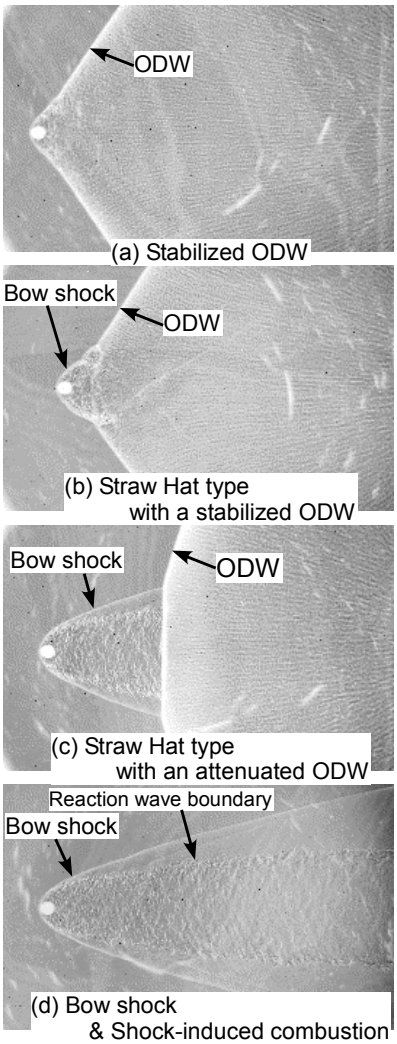

Figure 2. Snapshots of combustion regimes in $2H_2+O_2+3Ar$ mixture. Initial pressures were (a) 141kPa, (b) 136kPa, (c) 131kPa and (d) 121kPa.

4 Results and Discussion: Critical curvature radiuses for curved detonation waves

In the previous studies [16, 17], we focused on the critical conditions between the stabilized ODW (figure 2(a)) and the Straw Hat type with a stabilized ODW (figure2 (b)). These two regimes were distinguished as the stable or unstable wave structure. We concluded that the propagation limit of the curvature effect will be responsible for this criticality, by carefully processing the camera pictures of the stabilized ODW just above the criticality (critical mode). We extracted the wave shapes from the camera images, and applied the fitting function to them. For the stabilized ODW having the stable wave structure, this procedure allowed us to calculate the whole distributions of wave angle (propagation velocity) and curvature radius by using the projectile velocity and the first and second derivatives of the function. Because of the three-dimensional wave structure, the curvature radius was defined in the two components. We showed that the curvature radiuses at the local minimum point of wave propagation velocity became the one component (another component became infinity), and this curvature radius represents the critical curvature radius of curved self-sustained detonation.

In this paper, we focus on this critical mode of the stabilized ODW for the small projectile. Figure 4 shows distributions of wave propagation velocities on the crical mode of stabilized ODW for the small and large projectiles in $2H_2+O_2+3Ar$ mixture. Horizontal axis represents the vertical location on the wave from the center of spherical projectile. Vertical axis is the propagation velocity normalized by the C-J velocity. The wave velocity coincided with the projectile velocity at the projectile front ($y = 0$), and had the local minimum value at 0.8-0.9 D_{CJ} by the curvature effect before the wave velocity asymptotically reached the C-J velocity at far field. The vertical location where the wave velocity had the local minimum value was smaller for the small projectile than that for the large projectile. We defined the curvature radiuses as R_1^* on these points. In figure 5, the R_1^* for the small and large projectile is plotted against V_p / D_{CJ} in various mixture compositions. Although the dispersions of V_p / D_{CJ} existed, our previous study [16] showed the R_1^* had almost constant value in the range of V_p / D_{CJ}

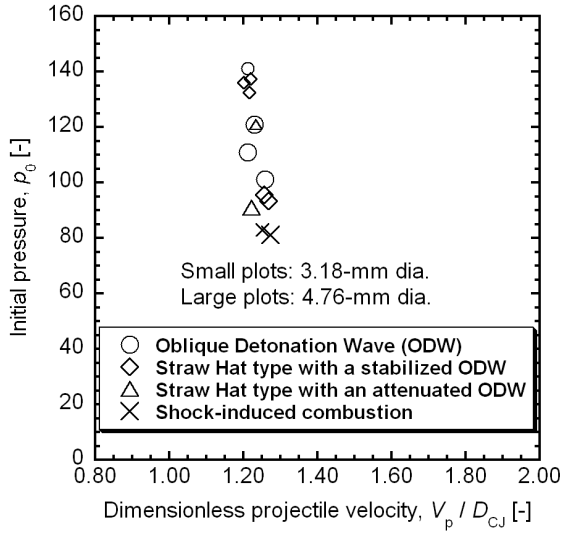

Figure 3. Observed combustion regimes in $2H_2$+O_2+3Ar mixture (comparison between the small and large projectile).

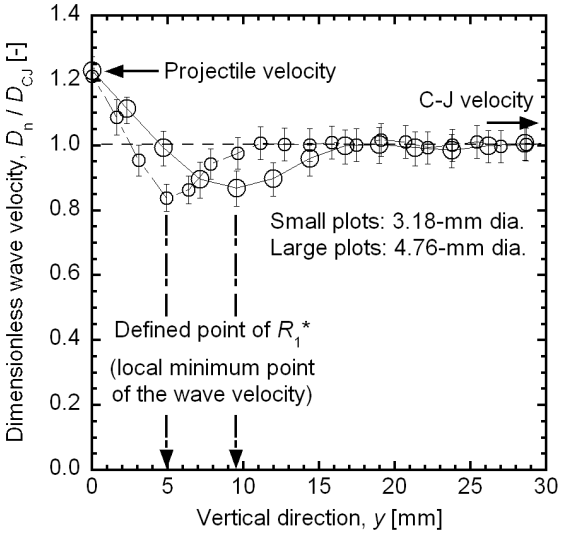

Figure 4. Distributions of the propagation velocity on the stabilized ODW in the critical mode using $2H_2$+O_2+3Ar mixture (comparison between the small and large projectile).

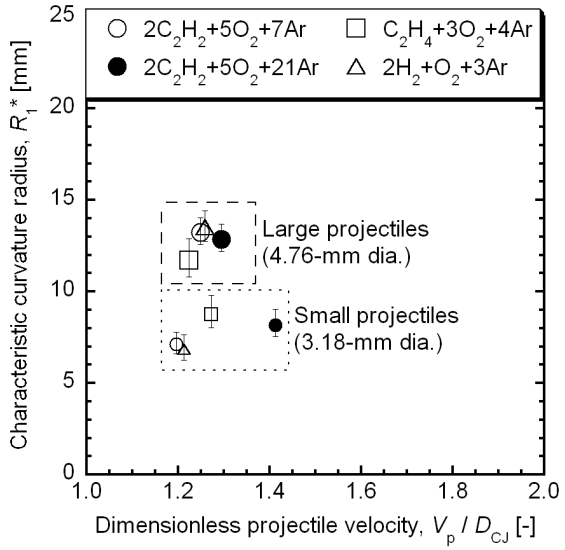

Figure 5. The curvature radiuses where the wave velocity had the local minimum value in the critical mode of stabilized ODW.

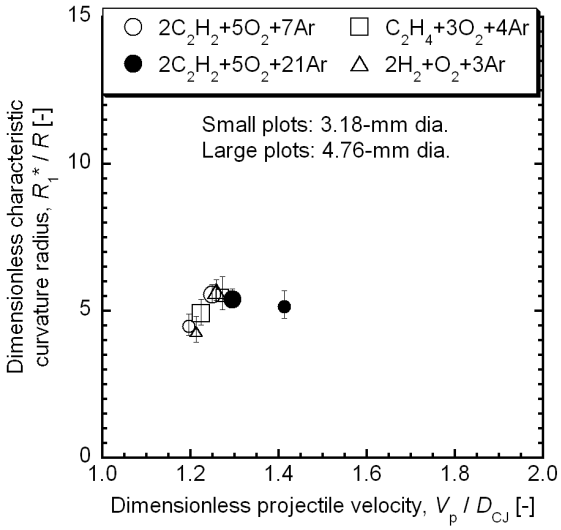

Figure 6. The R_1^* normalized by the projectile radiuses in the critical mode of stabilized ODW.

= 1.1-1.8. Therefore, we discuss the effects of projectile scales and mixture compositions in figure 5. The R_1^* in the critical mode was about 8 mm and 13 mm for the small and large projectiles, respectively, regardless of the mixture compositions. Figure 6 shows the R_1^* normalized by the projectile radiuses (1.6mm and 2.4mm for the small and large projectile, respectively). The R_1^* was almost proportional to the projecitle radius, and was about 5 times of it. Figure 7 shows the R_1^* normalized by the cell sizes of the planar detonations in each experimental condition. Regardless of the projectile radiuses, the R_1^* was about 8-10 times and 15 times the cell sizes for mixtures diluted with 50% and 75% argon, respectively. Figures 6 and 7 represent two characteristics of the R_1^* in the critical mode of stabilized ODW. Firstly, the projectile radius (diameter) proportionally affects the geometrical scale (R_1^*) of the wave around the projectile. Secondly, the fraction of mixture dilution affects the required cell sizes to sustain the curved detonation wave which has the curvature radius R_1^*.

Finally, in figure 8, the observed combustion regimes are plotted for the small projectile in various mixture compositions. Note that the results of the mixtures with 50% dilution are represented in the

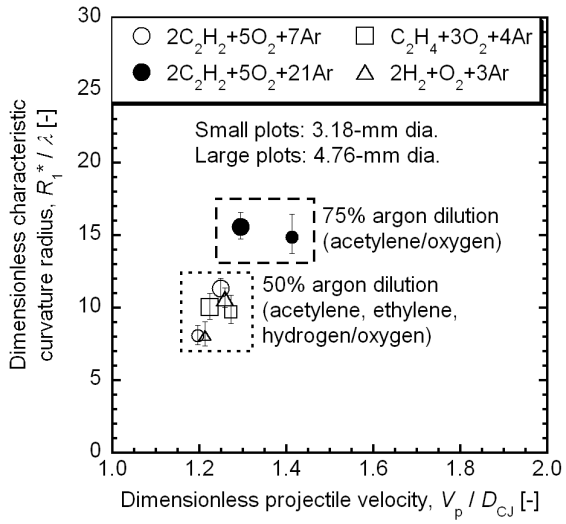

Figure 7. The R_1^* normalized by the cell size in the critical mode of stabilized ODW.

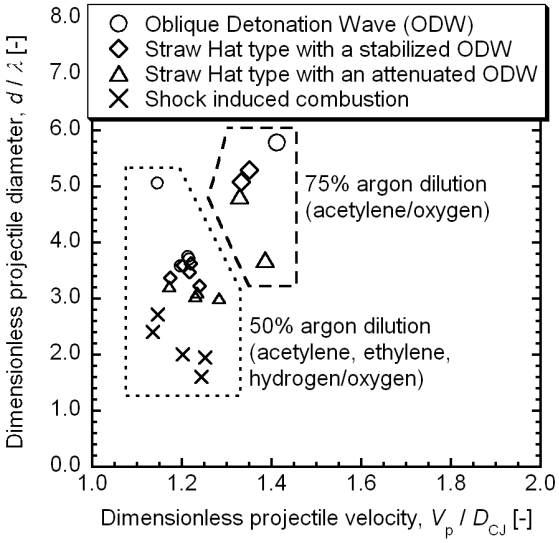

Figure 8. Combustion regimes for the small projectile in invarious mixture compositions.

same symbols. The vertical axis is expressed as the dimensionless projectile diameter, d / λ as in previous studies [5, 7, 8, 14-17]. The criticalities for stabilizing the ODW were about $d / \lambda = 3.5$ and 5.5 for the mixture with 50% and 75% dilution, respectively. These results agreed with the results of large projectiles obtained in our previous studies [14-17]. This indicates the dimensionless projectile diameter is a unique parameter for the stabilizing criticality regardless of the projectile diameter.

5 Conclusions

Stabilizations of oblique detonation waves by sphere projectiles were investigated using smaller projectiles (3.18-mm dia.) than that (4.76-mm dia.) used in our previous studies.

The combustion regimes shifted as the stabilized ODW, Straw Hat type with a stabilized ODW, Straw Hat type with an attenuated ODW and shock-induced combustion, as the initial pressure of the mixture decreased. The qualitative trend was almost the same as that using the large projectiles.

In the critical mode of stabilized ODW, the wave velocity distribution had the local minimum value (0.8-0.9 times the C-J velocity) by the curvature effect. The wave curvature radius (R_1^*) on this characteristic point was about 5 times the projectile radius, regardless of the mixture composition. The curvature radius normalized by the cell sizes was about 8-10 and 15 for mixtures diluted with 50% and 75% argon, respectively. These dimensionless curvature radiuses agreed with those of the large projecitles.

The stabilizing criticality expressed by the dimensionless projectile diameter (d / λ) was about 3.5 and 5.5 for mixtures diluted with 50% and 75% argon, respectively. These criticalities agreed with those of the large projectiles.

Acknowledgements

This work was subsidized by the Ministry of Education, Culture, Sports, Science and Technology via a Grant-in-Aid for Scientific Research (A), No. 20241040; a Grant-in-Aid for Scientific Research (B), No. 21360411; and the Research Grant Program from the Institute of Space and Astronautical Science, the Japan Aerospace Exploration Agency.

References

[1] Lehr, H.F.: Experiments on shock-induced combustion. Astronaut. Acta. **17**(4, 5), 589-597 (1972)

[2] Chernyavskii, S.Yu., Baulin, N.N. and Mkrtumov, A.S.: High-speed flow of a mixture of hydrogen and oxygen over blunt bodies. Combust. Expl. Shock Waves **9**, 687-690 (1973)

[3] Hertzberg, A., Bruckner, A.P. and Bogdanoff, D.W.: Ram accelerator: A new chemical method for accelerating projectiles to ultrahigh velocities. AIAA J. **26**(2), 195-203 (1988)

[4] Powers, J.M.: Combustion in High-Speed Flows, Kluwer Academic Publishers, Boston, 345-371 (1994)

[5] Lee, J.H.S.: Initiation of detonation by a hypervelocity projectile. Prog. Astronaut. Aeronaut. **173**, 293-310 (1997)

[6] Vasiljev, A.A.: Initiation of gaseous detonation by a high speed body. Shock Waves **3**, 321-326 (1994)

[7] Higgins, A.J. and Bruckner, A.P.: Experimental investigation of detonation initiation by hypervelocity blunt projectiles. AIAA paper 96-0342 (1996)

[8] Kasahara, J., Arai, T., Chiba, S., Takazawa, K., Tanahashi, Y. and Matsuo, A.: Criticality for stabilized oblique detonation waves around spherical bodies in acetylene/oxygen/krypton mixtures. Proc. Combust. Inst. **29**, 2817-2824 (2002)

[9] Kaneshige, M.J. and Shepherd, J.E.: Oblique detonation stabilized on a hypervelocity projectile. Twenty-Sixth Symposium (International) on Combustion, 3015-3022 (1996)

[10] Verreault, J. and Higgins, A.J.: Initiation of detonation by conical projectiles. Proc. Combusti. Inst. **33**, 2311-2318 (2011)

[11] Li, C., Kailasanath, K. and Oran, E.S.: Detonation structures behind oblique shocks. Phys. Fluids **6**(4), 1600-1611 (1994)

[12] Choi, J.-Y., Shin, E.J.-R. and Jeung, I.-S.: Unstable combustion induced by oblique shock waves at the non-attaching condition of the oblique detonation wave. Proc. Combusti. Inst. **32**, 2387-2396 (2009)

[13] Kasahara, J., Fujiwara, T., Endo, T. and Arai, T.: Chapman-Jouget oblique detonation structure around hypersonic projectiles. AIAA J. **39**(8), 1553-1561 (2001)

[14] Maeda, S., Inada, R., Kasahara, J. and Matsuo, A.: Visualization of the non-steady state oblique detonation wave phenomena around hypersonic spherical projectile. Proc. Combust. Inst. **33**, 2343-2349 (2011)

[15] Maeda, S., Kasahara, J. and Matsuo, A.: Oblique detonation wave stability around a spherical projectile by a high time resolution optical observation. Combust. Flame **159**(2), 887-896 (2012)

[16] Maeda, S., Kasahara, J. and Matsuo, A.: Unsteady propagation process of oblique detonation waves initiated by hypersonic spherical projectiles. Trans. JSASS Aerospace Tech. Japan **10**(ists28), Pe_1-Pe_6 (2012)

[17] Maeda, S., Sumiya, S., Kasahara, J. and Matsuo, A.: Initiation and sustaining mechanisms of stabilized oblique detonation waves around projectiles. Proc. Combust. Inst. **34**, 1973-1980 (2013)

[18] Kaneshige, M., Shepherd, J.E.: Detonation database, GALCIT Technical Report FM97-8. http://www.galcit.caltech.edu/detn_db/html/ (1997)

[19] Reynolds, W.C.: The Element Potential Method for Chemical Equilibrium Analysis: Implementation in the Interactive Program STANJAN: Version 3. Technical Report No. A-3991, Stanford Univ. (1986)